J Appl Electrochem (2010) 40:653–662
DOI 10.1007/s10800-009-0040-y

ORIGINAL PAPER

Electrochemical behavior of copper current collector in imidazolium-based ionic liquid electrolytes

Chengxin Peng · Li Yang · Shaohua Fang · Jixian Wang · Zhengxi Zhang · Kazuhiro Tachibana · Yong Yang · Shiyong Zhao

Received: 11 June 2009 / Accepted: 23 November 2009 / Published online: 10 December 2009

Abstract The electrochemical behaviors of copper current collector in 1-alkyl-3-methylimidazolium bis[(trifluoromethyl)sulfonyl] imide ionic liquid electrolytes were investigated and compared with that in ethylene carbonate/dimethyl carbonate solutions. Cyclic voltammetry results showed that large oxidation–reduction current of the copper foil appeared in ethylene carbonate/dimethyl carbonate solutions, while a much smaller current in the room temperature ionic liquid electrolytes decreased gradually, indicating that the copper foil was anodically stable. Further study by X-ray photoelectron spectroscopy analysis showed that an unstable product was composed mainly of the carbonate and carbonyl species on the surface of the copper foil after the electrochemical measurement in ethylene carbonate/dimethyl carbonate solutions, leading to the dissolution of the copper foil. While a better passivating film from the reduction of the anions in the room temperature ionic liquid electrolytes covered the surface of copper foil and protected the copper foil from being oxidized even in a higher potential. These results indicate that the use of room temperature ionic liquid electrolytes can improve the stability of copper current collector in the advanced lithium ion batteries.

Keywords Lithium ion battery · Copper current collector · Corrosion · Ionic liquid · Electrolytes

C. Peng
The Institute for Advanced Materials and Nano Biomedicine, Tongji University, Shanghai 200092, China

L. Yang (✉) · S. Fang · J. Wang · Z. Zhang
School of Chemistry and Chemical Technology, Shanghai Jiao Tong University, Shanghai 200240, China
e-mail: liyangce@sjtu.edu.cn

K. Tachibana
Department of Chemistry and Chemical Engineering, Yamagata University, Yamagata 992-8510, Japan

Y. Yang
State Key Lab of Physical Chemistry of Solid Surface, Xiamen University, Xiamen 361005, China

S. Zhao
Zhangjiagang Green Battery Material Research Institute Co. Ltd, Zhangjiagang 215600, China

1 Introduction

Copper (Cu) is commonly used as the anodic current collector for negative electrodes in lithium ion batteries. It plays an important role in exchanging electrons between the electrode materials and the external circuit. However, Cu current collector may be subjected to the corrosion during the charge/discharge processes, which can degrade the performance and worsen the safety of lithium ion batteries. P. Arora et al. [1] have summarized the capacity fading mechanisms in lithium ion batteries including the dissolution of Cu current collector. Further research [2] by Yang et al. showed that the dissolved Cu ions from the current collector precipitated as Cu oxides on the carbon surface, which blocked the normal intercalation of lithium ions and led to the capacity fading of lithium ion batteries. Besides, Aurbach and Cohen [3] suggested that copper in $LiAsF_6$-PC was not completely inert at open-circuit potential (OCP) and contaminants might oxidize the copper. Also, Zhao et al. [4] have reported that the dissolution of copper in ternary organic mixture containing $LiPF_6$ appeared at about 3.5 V versus Li^+/Li, which was less than 0.5 V above the OCP of the electrode. Although other study has described that the corrosion of copper could not

be realized on the negative electrode on account of that the upper limit of its potential is estimated to be 1.5 V versus Li^+/Li in most practical uses of the commercial lithium ion batteries [5], the dissolution of Cu current collector is still inevitable to occur during the overdischarged process [4], especially for lithium ion batteries with high voltage cathodic materials [6], the copper current collector for negative electrodes may reach a potential high enough to be corroded at the end of the discharge process. Therefore, it is necessary to investigate the stability of copper current collector in the electrolytes which is used to improve the performance of lithium ion battery.

Organic-based electrolytes have been widely used in lithium ion batteries. Owing to their flammability and volatility, their use in lithium ion battery is limited, especially for those advanced lithium ion batteries used as the power source of the electric vehicle (EV) and other large-scale power systems [7, 8]. Recently, room temperature ionic liquids (RTILs) have received considerable attentions due to their excellent properties, such as high thermal stability, nonflammability, low vapor pressure, and wide electrochemical window [9–14], etc. Among these RTILs, the imidazolium-based room temperature ionic liquids are most commonly used owing to their relatively easy synthesis, considerable ion conductivity as 10^{-2} S cm^{-1} and so on. Besides, lithium bis[(trifluoromethyl)sulfonyl] imide [$LiN(CF_3SO_2)_2$, LiTFSI] salt has great thermal, hydrolytic stability, good conductivity, and high electrochemical stability. These RTILs containing LiTFSI can be potentially used as a good candidate for lithium ion batteries [15–17]. However, up to now, there were few reports studying the current collector behaviors in these RTIL electrolytes. In the previous report, we have showed that the Al cathode current collector was stable in a series of 1-alkyl-3-methylimidazolium bis[(trifluoromethyl) sulfonyl] imide ionic liquid electrolytes [18], whereas the electrochemical behaviors of the Cu anode current collector in these RTIL electrolytes are still unclear.

In this article, the electrochemical behaviors of the Cu current collector were studied in 1-alkyl-3-methylimidazolium bis[(trifluoromethyl)sulfonyl] imide ionic liquid electrolytes. The results were compared with that in ethylene carbonate (EC)/dimethyl carbonate (DMC) solutions to find more suitable electrolytes with better compatibility between the RTILs and Cu current collector. In this study, cyclic voltammetry (CV), scanning electron microscopy (SEM), and X-ray photoelectron spectroscopy (XPS) were used for characterization.

2 Experimental

LiTFSI salt (99.9%, Morita) was dried under vacuum at 120 °C for 24 h prior to use. Room temperature ionic liquids based on $TFSI^-$ anion, 1-ethyl-3-methylimidazolium bis[(trifluoromethyl)sulfonyl] imide (EMI-TFSI), and 1-butyl-3-methylimidazolium bis[(trifluoromethyl)sulfonyl] imide (BMI-TFSI) were prepared in our laboratory according to the procedures in the previous studies [19, 20]. Before making solutions, these RTILs were treated with molecular sieves (4 Å) for 2 days to dehydrate so that water content in them was less than 30 ppm which was determined by Karl Fisher titration method (Fig. 1 shows their chemical structures). LiTFSI salt was dissolved in EMI-TFSI, BMI-TFSI, and EC/DMC (1:1 in vol., 98%, Zhangjiagang Guotai Huarong New Chemical Materials Co. Ltd.) to make 1 mol dm^{-3} (M) solutions, respectively.

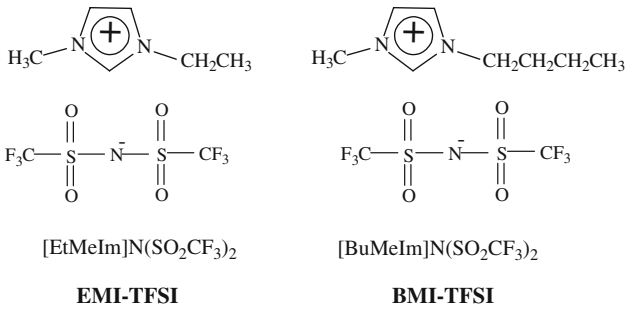

Fig. 1 Chemical structures of the RTILs

The electrochemical behaviors of the Cu current collector were investigated using CHI 604B electrochemical work-station (CH Instruments, USA). A standard cell (inner volume: 10 cm^3) with three isolated electrodes was applied in this experiment. A specimen of Cu foil (13 μm thickness, 99.9%) was cut into small pieces as tape electrodes with dimensions of 50 mm × 50 mm exposed to the electrolytes. After Cu foil was degreased in acetone for 30 min and dried at room temperature under vacuum, it was electropolished at an anodic constant potential of 2.0 V in a phosphoric acid solution for about 15 min. It was then rinsed thoroughly in a 10% phosphoric acid solution and deionized water. Finally, Cu foil was dried at room temperature under vacuum for 48 h. The treated copper foil, lithium foil, and lithium foil were used as working electrode, reference, and counter electrodes, respectively. Cyclic voltammetry of the copper foil in each electrolytes mentioned above was performed for three times with a potential scan rate of 10.0 mV s^{-1}. Before the experimental, the electrochemical windows of the electrolytes were tested using linear sweep voltammetry (LSV) under a scan rate of 10.0 mV s^{-1}. In this scan, a platinum (Pt) disk with 2 mm diameter and two pieces of Li foils were used as working electrode, reference, and counter electrodes, respectively. In this article, all potentials were relative to the standard potential of Li^+/Li. The electrolytes preparation processes and the electrochemical measurements were conducted in UNiLab glove box

($[O_2] < 20$ ppm, $[H_2O] < 20$ ppm) filled with argon (Ar) atmosphere at ambient temperature.

After the electrochemical measurements, the copper foils were well rinsed by the dimethyl carbonate (DMC) solvent and then dried at room temperature under vacuum for 24 h. These copper foils were then transferred in a portable sealed carrier from the Ar-filled glove box to the sample holder of SEM (LEO 1530, Oxford Instrument) chamber to observe their surface morphology.

X-ray photoelectron spectroscopy (XPS) measurement was applied to analyze the composition on the surface of copper foils after the electrochemical measurements. A sample preparation was conducted using a similar method with the SEM observation. The analysis chamber of XPS (Quantum 2000, Physical Electronics) was kept at 5×10^{-8} Pa and Al Kα line was used as an X-ray source which operated at 8 mA and 2 kV to obtain the spectra of each element existing on the surface of copper foils after the electrochemical measurements.

3 Results and discussion

3.1 Electrochemical behaviors of Cu foil electrode in the RTIL electrolytes and the EC/DMC solutions

In order to study the electrochemical behaviors of Cu foil in the electrolytes, the electrochemical windows of EC/DMC containing 1 M LiTFSI and the RTILs were tested at the beginning. As shown in Fig. 2, the reduction and the oxidation potentials of the RTILs occurred at around 1.5 and 6.0 V, while the corresponding potentials of the EC/DMC solutions were found at about 0.5 and 5.7 V, respectively. These results were in good agreement with the previous reports [18, 21]. Almost no current was observed obviously in the potential range of 1.5–5.5 V for above electrolytes, which indicated that no more electrolytes degradation considerably occurred.

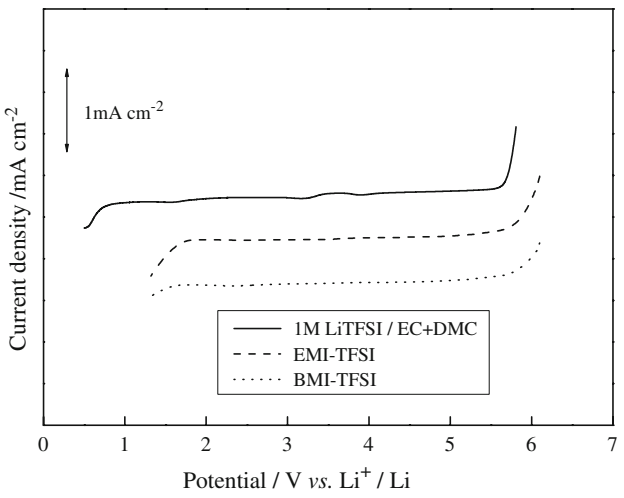

Fig. 2 Linear sweep voltammetry on platinum at EC/DMC containing 1 M LiTFSI and RTILs (sweep rate: 10.0 mV s^{-1})

Cyclic voltammetry (CV) was performed in the potential range of 1.5–5.5 V to investigate the electrochemical behaviors of the Cu current collector in the electrolytes. Figure 3 showed the anodic behaviors of the Cu foil in EC/DMC solutions and the RTILs containing 1 M LiTFSI. During the anodic potential sweep from 3.0 to 3.8 V, no more electrolytes degradation occurred obviously. While for the EC/DMC solutions shown in Fig. 3a, a sharp continuous current rise at about 3.5 V, which was ascribed to the oxidation of the Cu foil. In the reverse scan, the reduction of the Cu ion was observed at around 3.4 V [4, 22]. Similar results also appeared in $LiPF_6$ and $LiClO_4$-based electrolytes [4, 5]. These phenomena showed that copper current collector was prone to oxidation in the organic electrolytes at the potentials of around 3.5 V. Therefore, the potentials of negative electrodes in the batteries should be limited to about 3.5 V. Besides, the current density of the Cu foil in the EC/DMC solutions slightly increased during the following sweeps, which indicated that the Cu foil was not stable and its corrosion occurred in the EC/DMC solutions. It is disadvantageous because the dissolved copper will plate on surface of the carbon anode during the charge/discharge processes, leading to degradation of the performance of lithium ion batteries. For the RTIL electrolytes shown in Fig. 3b and c, a weaker anodic current at about 3.4 V was observed, compared with that of the EC/DMC solutions. It rapidly decreased during the following cycles, which suggested that the Cu foil was stable in the RTIL electrolytes. The reason was that a protective film might form on the surface of Cu foil in the RTIL electrolytes during the potential sweeps and it suppressed the oxidation of the Cu foil as a result. The stability of the Cu current collector in the RTIL electrolytes can improve the safety of lithium ion batteries during the charge/discharged processes, especially at an over-discharged state. For example, when a practical lithium ion battery containing $LiCoO_2$ was over-discharged to ~0.4 V, copper corrosion would occur in EC/DMC solutions while not in the RTIL electrolytes since the E_{anode} reached ~3.4 V, based on the fact that OCP of fully discharged Li_xCoO_2 is ~3.8 V [23].

Cyclic voltammetry was also performed to investigate the reduction of the electrolytes on the surface of the Cu foil during the cathodic scan. The voltammetric response of the Cu foil in EC/DMC solutions from 3.0 to 0.0 V was shown in Fig. 4a, obvious reduction peaks at around 0.3 and 0.8 V appeared, which were attributed to the reduction of the solvents in the electrolytes [24]. While the other reduction peaks at about 1.2 V was assigned to the

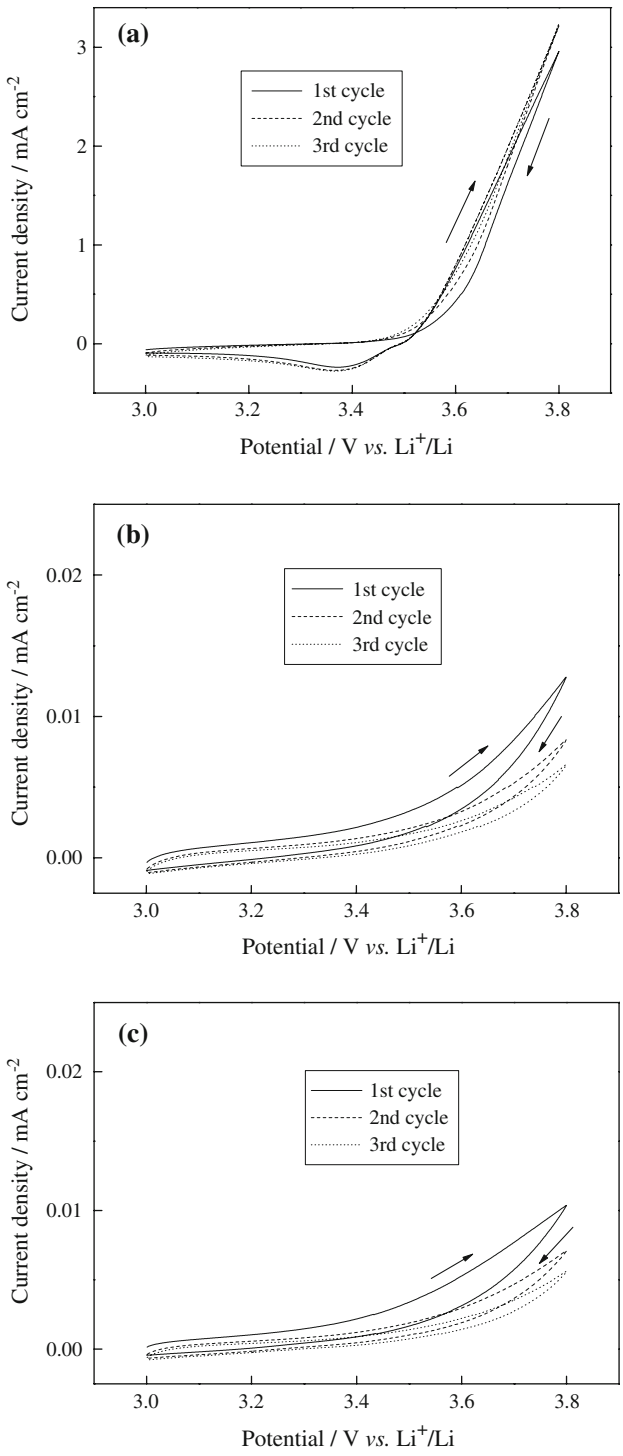

Fig. 3 Cyclic voltammograms for Cu foil electrode in 1 M LiTFSI–EC/DMC (**a**); 1 M LiTFSI–EMI-TFSI (**b**); 1 M LiTFSI–BMI-TFSI (**c**) (sweep potential range: 3.0–3.8 V; scan rate: 10.0 mV s^{-1})

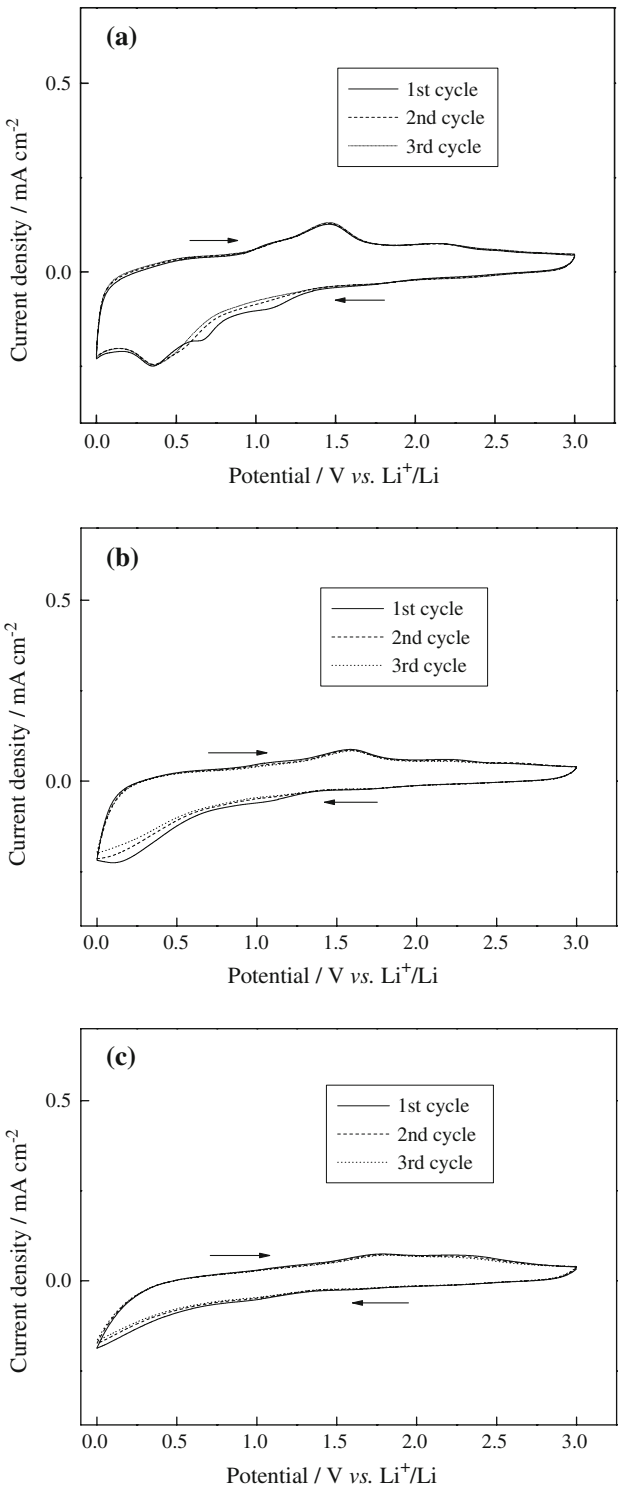

Fig. 4 Cyclic voltammograms for Cu foil electrode in 1 M LiTFSI–EC/DMC (**a**); 1 M LiTFSI–EMI-TFSI (**b**); 1 M LiTFSI–BMI-TFSI (**c**) (sweep potential range: 3.0–0.0 V; scan rate: 10.0 mV s^{-1})

reduction of residual moisture in the electrolytes [25]. When the potential reached 0.0 V, a reduction peak was observed, which was followed by a very small oxidation peak at about 1.0 V and a broad peak near 1.5 V in the reverse scan. Compared with that in the RTIL electrolytes shown in Fig. 4b and c, the oxidation peak at around 1.0 V was absent in the RTIL electrolytes, indicating that this oxidation peak might be ascribed to the reverse reaction of the reduction products of the solvents at 0.3 and 0.8 V.

Besides, the other typical peaks at 0.0 V and ~1.5 V appeared during the potential sweeps in the RTIL electrolytes. The peak at 0.0 V might not be assigned to the reduction of the lithium ion because the dissolution of lithium in the EMI-TFSI electrolytes happened at −0.5 V. Moreover, the oxidation peak of lithium ion at the potential of ~0.25 V did not present in the reverse scan [26]. Consequently, these two peaks might be related to the reduction and the reverse reaction of the reduction products of $N(SO_2CF_3)_2^-$ anion which existed in both electrolytes. The peak at around 2.0 V in both kinds of electrolytes systems was ascribed to the oxidation of the Cu to Cu^+ [27]. The different CV features of the Cu foil in the RTIL electrolytes and EC/DMC solutions suggested that almost no electrolytes degraded greatly during the potential sweeps in the RTIL electrolytes, which may be useful to enhance the safety of lithium ion batteries, especially at an over-charged state.

In oreder to further evaluate the influence of the reduction of the electrolytes on the electrochemical behaviors of the Cu current collector, the CVs of the Cu foil both in the EC/DMC solutions and in the RTIL electrolytes were carried out during the potential swept from 0.0 to 3.8 V. In the EC/DMC solutions, it was observed that the anodic peak of the Cu foil at the potential around 3.5 V decreased gradually with the continual cycles (Fig. 5a), which was opposite to the continuous increasing CV features of the Cu foil in the same electrolytes during the potential swept from 3.0 to 3.8 V. According to the results from the preliminary experiments, no decreasing tendency of the Cu oxidation peak near 3.5 V took place during the cathodic scan with different switch potentials until the reduction peaks appeared at around 0.3 and 0.8 V. These phenomena revealed that some amounts of electrolytes reduced and formed some protection on the Cu foil. These passivating film attenuated the further oxidation of the Cu foil and thus the oxidation current of the Cu foil at around 3.5 V decreased. Zhao et al. [4] have also showed similar results that the passivating film formed on the copper foil and gave some protection to suppress its oxidation in ternary organic mixture containing $LiPF_6$. Figure 5b and c showed the CVs of the Cu foil in the RTIL electrolytes. A weaker oxidation current of the Cu foil electrode in both RTIL electrolytes was observed compared with that in the EC/DMC solutions, indicating that a better film formed on the Cu foil electrode which inhibited the further oxidation of the Cu foil. These results confirmed that the reduction of the electrolytes during the potential sweeps might provide some protection for Cu current collector for lithium ion batteries.

In order to examine the stability of the protection formed on the Cu foil during the potential sweeps in EC/DMC solutions and the RTIL electrolytes, the potential

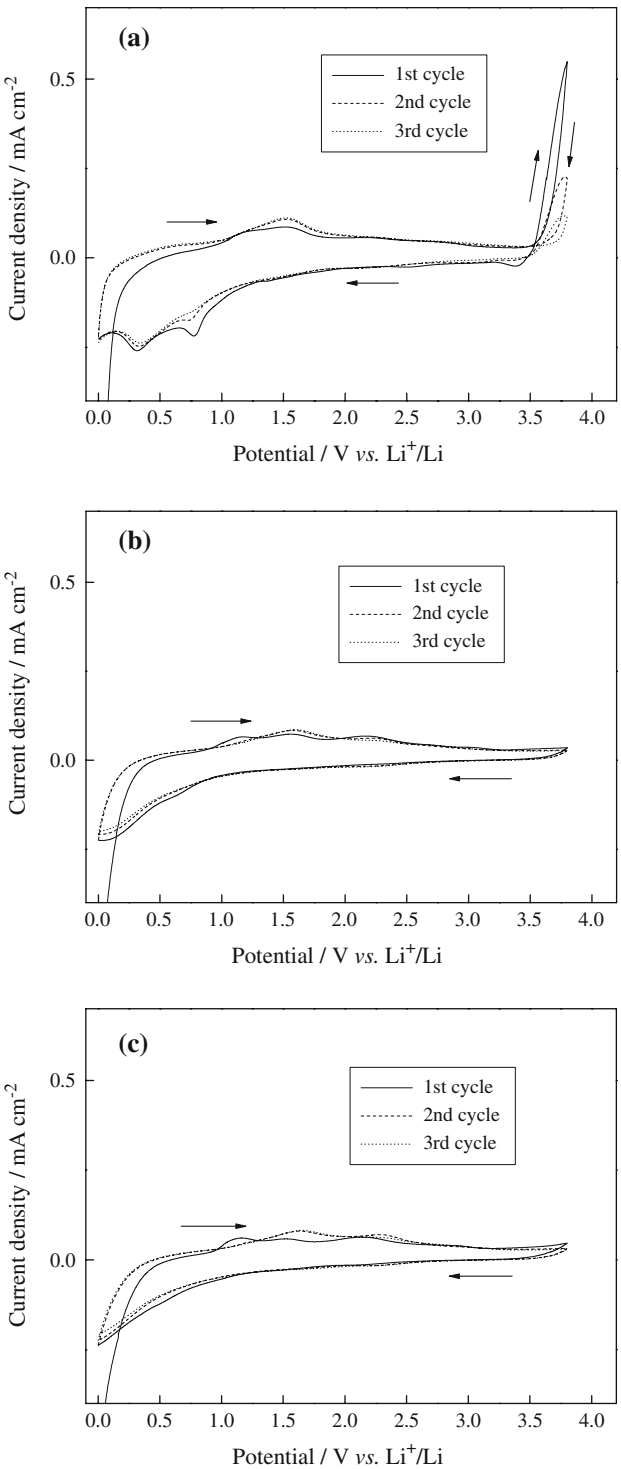

Fig. 5 Cyclic voltammograms for Cu foil electrode in 1 M LiTFSI–EC/DMC (**a**); 1 M LiTFSI–EMI-TFSI (**b**); 1 M LiTFSI–BMI-TFSI (**c**) (sweep potential range: 0.0–3.8 V; scan rate: 10.0 mV s^{-1})

swept positively to 5.0 V. In the EC/DMC solutions, an oxidation current of the Cu foil increased rapidly at about 4.0 V in the first cycle (Fig. 6a), implying the dissolution of copper occurred on the Cu foil. However, a higher

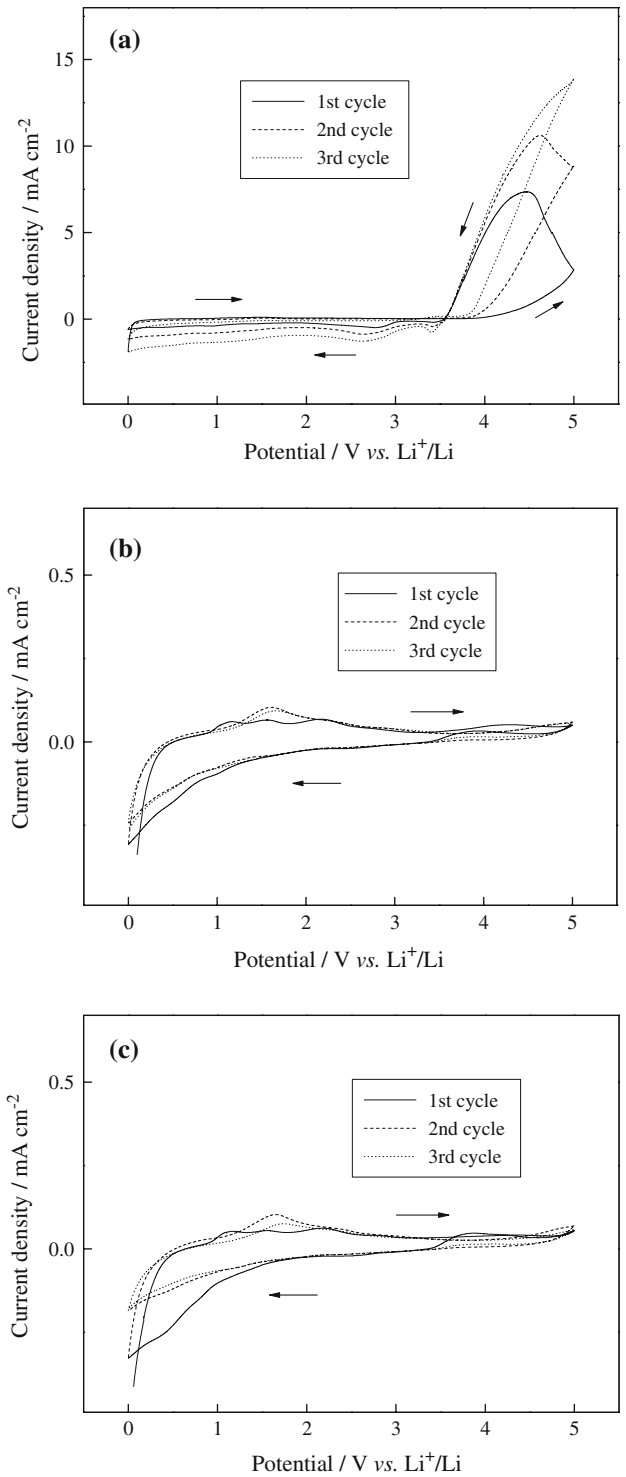

Fig. 6 Cyclic voltammograms for Cu foil electrode in 1 M LiTFSI–EC/DMC (**a**); 1 M LiTFSI–EMI-TFSI (**b**); 1 M LiTFSI–BMI-TFSI (**c**) (sweep potential range: 0.0–5.0 V; scan rate: 10.0 mV s^{-1})

oxidation current occurred during the reverse potential scans showed that the process was accompanied by a corrosion step on the surface of the Cu foil. In the continuous cycles, the magnitude of the oxidation current increased and the corrosion potential simultaneously shifted negatively to a lower potential. These behaviors suggested that a less effective protection film formed on the surface of the Cu foil. Thus, it was prone to the breakdown and the dissolution of the Cu foil appeared. In the experiment, it was observed that the Cu foil was broken down and large amounts of pits appeared on its surface after five potential scans, indicating that serious Cu foil corrosion occurred during the potential sweeps in the EC/DMC solutions. Although the reduction of the electrolytes had provided the limited protection for the Cu foil, the protective film was not stable and not enough to protect the Cu foil from being eroded at the higher voltage. Whereas, in the RTIL electrolytes, it was found that a weaker oxidation current of the Cu foil presented and it decreased with the following cycles. The oxidation current was less than 0.05 mA cm^{-2}, much smaller than that in the EC/DMC solutions. This is because the stable protective film on the surface of the Cu foil, which came from the reduction of the RTIL electrolytes during the cathodic scan, inhibited the dissolution of the Cu foil even the potential up to 5.0 V. Besides, similar shape of cyclic voltammograms of the Cu foil suggested that the electrochemical behaviors on the Cu foil were essentially same in both RTIL electrolytes. Therefore, it can be concluded that the Cu foil is completely passivated in the RTIL electrolytes which can resist higher anodic potential. The high stability of copper current collector in the RTIL electrolytes can be available to improve the safety of lithium ion batteries during the overcharged process, especially for the stacks of batteries during the reverse-charged state when some individual cell encountered the mistaken way in the assemble processes.

3.2 Morphology of Cu foil electrode after the electrochemical measurement

In order to investigate the formation of the passivating film more clearly, the morphology of the Cu foil was observed by SEM after multiple CV scans in the EC/DMC solutions and the RTIL electrolytes. In addition, the morphology of a raw copper foil (Fig. 7d) was also taken as a reference. Figure 7a–c showed the SEM images of the Cu foil after the potential sweeps from 0.0 to 3.8 V in the EC/DMC solutions and the RTIL electrolytes. As shown in Fig. 7a, some pits of 5–15 μm size were observed on the surface of the Cu foil, indicating that the dissolution of the Cu foil took place in the EC/DMC solutions, which led to the rise of anodic current during the potential swept to about 3.5 V. On the other hand, some solid products still formed on the Cu foil surface after the potential scans in the EC/DMC solutions. These compounds came from the reduction of the electrolytes during the potential sweeps, and played a role in attenuating the further corrosion of the Cu foil and

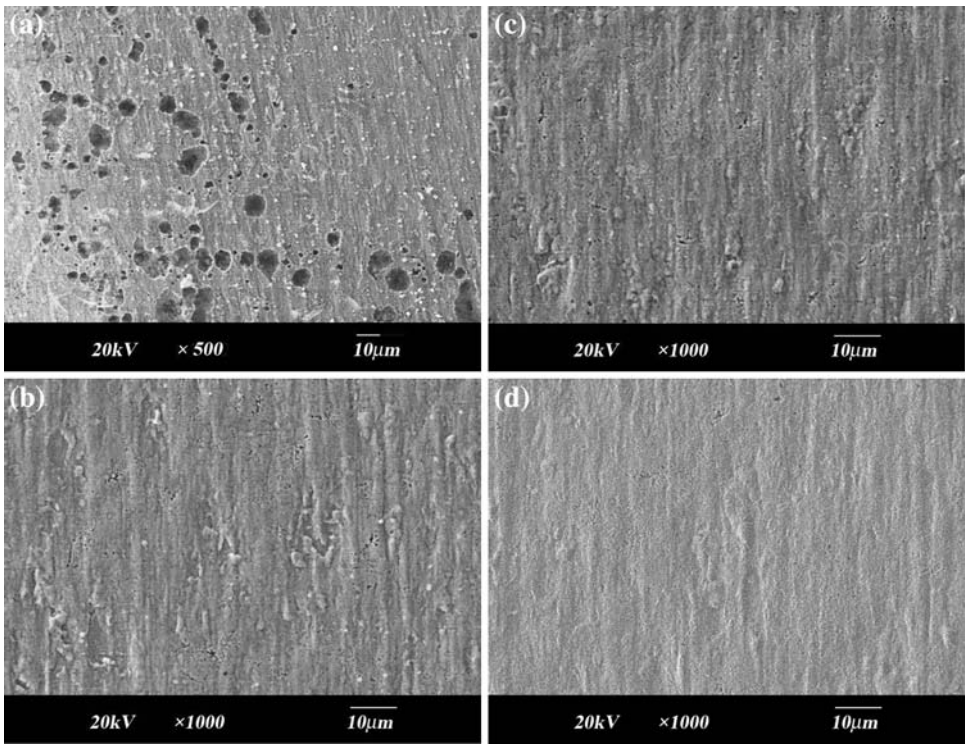

Fig. 7 SEM images of Cu foil electrode surface after the potential scanning from 0.0 to 3.8 V in 1 M LiTFSI–EC/DMC (**a**); 1 M LiTFSI–EMI-TFSI (**b**); 1 M LiTFSI–BMI-TFSI (**c**) and raw copper foil (**d**)

induced the decrease of the oxidation current at about 3.5 V during the potential sweeps from 0.0 to 3.8 V. However, this limited protective film was not stable enough to protect the Cu foil from its corrosion over higher potential. While for both EMI-TFSI and BMI-TFSI electrolytes, morphologies of the copper foils (Fig. 7b and c) showed that a deposited products film was formed on the Cu foil substrate after the potential sweeps, which protected the Cu foil electrode from its further oxidation. As a result, almost no obvious oxidation current of the Cu foil was observed from the above CV response. This obeservation indicated that the Cu foil surface was wholly passivated in both RTIL electrolytes after the electrochemical measurements. Based on the above results, it can be concluded that the above SEM images are in good agreement with the CV results. Although the protection behaviors for the Cu foil electrode were all observed in EC/DMC solution and RTIL electrolytes, higher oxidation current of the Cu foil in the EC/DMC electrolyte than that in the RTIL electrolytes, indicating that the dissolution of the Cu foil still existed in EC/DMC solution and it competed with the limited protection of the passivating film on the Cu foil. Once the protection for the Cu foil did not suppress the oxidation of the Cu foil, the copper corrosion happened. In comparison, a better passivating film formed in both EMI-TFSI and BMI-TFSI electrolytes, which was available to protect the Cu foil from its further oxidation.

3.3 Character of the Cu foil surface after the electrochemical measurement

In order to understand the complicated mechanism of corrosion and passivation processes, the passivating film on the Cu foil was analyzed by XPS measurement after the electrochemical measurement in EC/DMC solutions and the RTIL electrolytes. Additionally, high-resolution region spectra were obtained by a least-square fitting of model curve (XPSPEAK Version 4.0 software) after the removal of Shirley-type background.

Figure 8 showed the XPS spectra of C_{1s}, O_{1s}, N_{1s}, F_{1s}, Cu_{2p}, and S_{2p} for the Cu foil after the potential sweeps from 0.0 to 3.8 V in three electrolytes, and the XPS binding energies were summarized in Table 1. According to the XPS spectra, the most difference between the EC/DMC solutions and the RTIL electrolytes was the signal of C_{1s} and O_{1s} spectra. As for the C_{1s} spectra, the presence of species associated with C–C/C–H at 285.0 eV, C–O at 286.6 eV, and CO_3^{2-} or $ROCO_2Li$ at 289.0 eV [28] were found in all three electrolytes. However, the intensity of C_{1s} peak at 289.0 eV was higher in the EC/DMC solutions than that in the RTIL electrolytes, showing that almost no oxalates presented on the Cu foil surface after the potential sweeps in both RTIL electrolytes. Several mechanisms in following Eqs. 1–3 have been reported to explain their formation [29]. In the EC/DMC solutions, some solvents (such as EC and

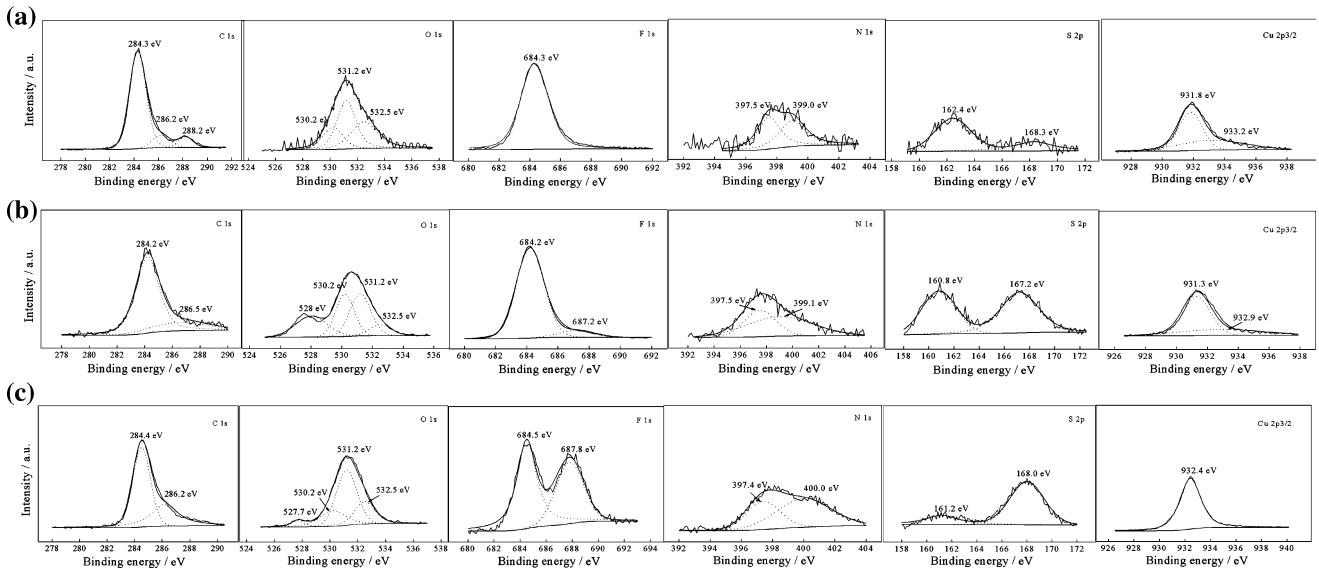

Fig. 8 XPS spectra for Cu foil electrode after the potential scanning from 0.0 to 3.8 V in 1 M LiTFSI–EC/DMC (**a**); 1 M LiTFSI–EMI-TFSI (**b**); 1 M LiTFSI–BMI-TFSI (**c**)

DMC) and their reduction products (Li_2CO_3 and CH_3O-CO_2Li) accounted for the appearance of three C_{1s} peaks, while only the C_{1s} peaks at 285.0 and 286.6 eV suggested the residual of DMC solvent after the rising process on the surface of the Cu foil in the RTIL electrolytes.

$$\text{EC: } (CH_2O)_2CO + 2e^- + 2Li^+ \rightarrow Li_2CO_3 + C_2H_4 \quad (1)$$

$$\text{DMC: } CH_3OCO_2CH_3 + 2e^- + 2Li^+ \rightarrow Li_2CO_3 + C_2H_6 \quad (2)$$

$$\text{DMC: } 2CH_3OCO_2CH_3 + 2e^- + 2Li^+ \rightarrow 2CH_3OCO_2Li + C_2H_6 \quad (3)$$

Peaks presented in the O_{1s} high-resolution region spectrum were identified as CO_3^{2-} or SO_2 at 532.5 eV [30], C=O at 531.5 eV and Cu_2O or CuO at 530.2 eV [31]. These peaks were all observed on the surface of the Cu foil after the electrochemical measurement in three electrolytes. However, a newly XPS spectra peak at 528.5 eV, which was ascribed to Li_2O [32], appeared on the Cu foil surface during the potential sweeps in both EMI-TFSI and BMI-TFSI electrolytes. These results indicated that a significant quantity of Li_2O formed on the surface of the Cu foil after the electrochemical measurement in the RTIL electrolytes. Although the presence of Li_2O may increase the internal resistance which will adversely affect the battery performance, the stable Li_2O formed on the Cu foil surface may improve the stability of the protective film, which will facilitate Cu current collector to resist higher voltage.

In addition to the C_{1s} and O_{1s} spectra, other spectra also showed the difference among the three electrolytes. The F_{1s} high-resolution region spectra presented two peaks at 685.0 and 687.8 eV, which were identified to LiF and $-CF_3$, respectively [28]. The N_{1s} high-resolution region spectrum displayed two peaks corresponding to nitride at 397.5 eV and $NSO_2CF_3^-$ at 399.7 eV [33], and the S_{2p} high-resolution region spectrum showed the presence of a number of peaks which were mostly likely associated with elemental sulfur and lithium sulfide from 160–165 eV, oxidized sulfur species at 167.0 and 168.2 eV, and $SO_2CF_3^-$ species at 169.0 eV [30]. By comparing the XPS spectra, it can be observed that higher intensity of F_{1s} spectra peak at 687.8 eV and N_{1s} spectra peak at 399.7 eV presented in the RTIL electrolytes, showing that a larger amount of species containing $-CF_3$ and $NSO_2CF_3^-$ on the Cu foil. In addition, the content of the S_{2p} spectra at 169.0 eV assigned to $SO_2CF_3^-$ species increased in the RTIL electrolytes. The formation of the passivating products on the Cu foil was explained by several mechanisms [30] in the following Eqs. 4–7. Based on the above results, it was concluded that more amounts of Li_2O, CF_3SO_2Li, and CF_3SO_2NLi species were presented on the surface of the Cu foil after the potential sweeps in the RTIL electrolytes, the majority of which appeared to be the reduction products of the $N(SO_2CF_3)_2^-$ anion.

$$N(SO_2CF_3)_2^- + ne^- + (n+1)Li^+ \rightarrow Li_3N + Li_2S_2O_4 + LiF + C_2F_xLi_y \quad (4)$$

$$N(SO_2CF_3)_2^- + 2e^- + 3Li^+ \rightarrow Li_2NSO_2CF_3 + CF_3SO_2Li \quad (5)$$

$$Li_2S_2O_4 + 6e^- + 6Li^+ \rightarrow 2Li_2S + 4Li_2O \quad (6)$$

$$Li_2S_2O_4 + 4e^- + 4Li^+ \rightarrow Li_2SO_3 + Li_2S + Li_2O \quad (7)$$

The XPS Cu_{2p} spectra were also investigated to confirm the passivating film on the Cu foil substrate. In the $Cu_{2p\ 3/2}$ spectra, two obvious peaks for cuprous ion (Cu^+) at about

Table 1 Summary of XPS binding energies (eV) for Cu foil electrode after the potential scanning from 0.0 to 3.8 V in 1 M LiTFSI–EC/DMC (a); 1 M LiTFSI–EMI-TFSI (b); 1 M LiTFSI–BMI-TFSI (c)

	Binding energy (eV)										
	C_{1s}			O_{1s}			F_{1s}	N_{1s}	S_{2p}	$Cu_{2p\ 3/2}$	
(a) 1 M LiTFSI/EC + DMC	284.3	286.2	288.2	–	530.2	531.2	532.5	684.3	397.5	399.0	162.4	168.3	931.8	933.2
(b) 1 M LiTFSI/EMI-TFSI	284.2	286.5	–	528.0	530.2	531.2	532.5	684.2	687.2	397.5	399.1	160.8	167.2	931.3	932.9
(c) 1 M LiTFSI/BMI-TFSI	284.4	286.2	–	527.7	530.2	531.2	532.5	684.5	687.8	397.4	400.0	161.2	168.0	932.4	–

932.0 eV and cupric ion (Cu^{2+}) at around 933. 4 eV were obtained on the surface of the Cu foil after the anodic scan. However, the signal of the Cu^{2+} spectra diminished for the EC/DMC solutions and the EMI-TFSI electrolytes, and it was absent in the BMI-TFSI electrolytes. As mentioned in the previous reports [34], Cu^{+} is more likely formed than Cu^{2+} in a non-aqueous environment. Other research [5] also confirmed that the oxidized copper existed as a cuprous ion (Cu^{+}) in the organic electrolytes. Consequently, the protective film on the Cu foil surface mainly consisted of cuprous ion (Cu^{+}) species such as Cu_2O, Cu_2CO_3, or $Cu_2(COO)_2$ after the anodic sweeps in the three electrolytes, whereas the presence of cupric ion (Cu^{2+}) in the protective film may relate to the residual moisture in the electrolytes.

Overall, the XPS analysis results showed that the products on the surface of the Cu foil after the electrochemical measurement in three electrolytes was mainly composed of lithium salts and the cupreous species. In addition, the results indicated a clearly different electrochemical behaviors of the Cu foil between the LiTFSI–EC/DMC solutions and the LiTFSI–RTIL electrolytes. Carbonate and carbonyl species were present on the Cu foil electrode surface after the electrochemical measurement in the EC/DMC solutions and absent in the RTIL electrolytes. While a larger amount reduction products of the $N(SO_2CF_3)_2^-$ anion formed on the surface of the Cu foil in the RTIL electrolytes than that in the EC/DMC solutions. These results were explained as that the solvents (EC and DMC) were reduced earlier than the $N(SO_2CF_3)_2^-$ anion, which contributed to appearance of the main protective film on the surface of the Cu foil in the EC/DMC solutions, while the reduction products of the $N(SO_2CF_3)_2^-$ anion composed the passivating film on the surface of the Cu foil after the electrochemical measurement in the RTIL electrolytes. With the above CV and XPS results of the Cu foil after the potential swept to 5.0 V in two kinds of electrolytes, it can be concluded that these carbonate and carbonyl species on the surface of the Cu foil in the LiTFSI–EC/DMC solutions was not stable over 5.0 V and thus the dissolution of the Cu foil appeared, while the reduction products of the $N(SO_2CF_3)_2^-$ anion formed on the surface of the Cu foil after the potential sweeps in the RTIL electrolytes, providing a effective protection for Cu current collector to resist higher voltage for advanced lithium ion batteries.

4 Conclusion

The electrochemical behaviors of the copper foil in 1-alkyl-3-methylimidazolium bis[(trifluoromethyl)sulfonyl] imide room temperature ionic liquids (RTILs) and EC/DMC solutions containing LiTFSI were investigated. It

was found that the Cu foil displayed the oxidation–reduction behaviors at about 3.5 V in the EC/DMC solutions while it was passivated in the RTIL electrolytes. Moreover, the reduction of the electrolytes was also studied, showing that the reduction of the electrolytes provided a limited protection for the Cu foil after the electrochemical measurement in EC/DMC solutions, and it was not stable enough to suppress the further oxidation of the Cu foil when the potential swept to high potentials. In comparison, a better passivating film covered on the surface of the Cu foil in the RTIL electrolytes, which protected the Cu foil from being oxidized. Further research by XPS analysis showed that the solid products was mainly composed of the reduction products of the electrolytes such as carbonate and carbonyl species on the surface of the Cu foil after the electrochemical measurement in the EC/DMC solutions. Those solutions were not stable at the potential up to 5.0 V and thus the dissolution of the Cu foil appeared. Whereas a better passivating film, coming from the reduction of $(CF_3SO_2)_2N^-$ anion in the RTIL electrolytes, coated on the Cu foil surface wholly to remarkably inhibit its further oxidation and provided an effective protection for the copper foil to resist higher voltage. These results indicated that a good film-coating behavior of the Cu foil presented in the RTIL electrolytes, which can improve the stability of copper current collector for advanced lithium ion batteries.

Acknowledgments The authors thank the research center of analysis and measurement of Shanghai Jiao Tong University for the help on the SEM measurements. This study was sponsored by the National Grand Fundamental Research 973 Program of China under Grant No. 2006CB202600, the National High Technology Research and Development Plan of China under Grant No. 2007AA03Z222.

References

1. Arora P, White RE, Doyle M (1998) J Electrochem Soc 145:3647
2. Yang L, Takahashi M, Wang B (2006) Electrochim Acta 5:3228
3. Aurbach D, Cohen Y (1997) J Electrochem Soc 144:3355
4. Zhao M, Kariuki S, Dewald HD, Lemke FR, Staniewicz RJ, Plichta EJ, Marsh RA (2000) J Electrochem Soc 147:2874
5. Kawakita J, Kobayashi K (2001) J Power Sources 101:47
6. Hyams TC, Go J, Devine TM (2007) J Electrochem Soc 154:C390
7. Liaw BY, Dubarry M (2007) J Power Sources 174:76
8. Terada N, Yanagi T, Arai S, Yoshikawa M, Ohta K, Nakajima N, Yanai A, Arai N (2001) J Power Sources 100:80
9. Blanchard LA, Hancu D, Beckman EJ, Brennecke JF (1999) Nature 399:28
10. MacFarlane DR, Huang JH, Forsyth M (1999) Nature 402:792
11. Endres F, Abedin SZE (2006) Phys Chem Chem Phys 82:101
12. Zhou ZB, Matsumoto H, Tatsumi K (2004) Chem Eur J 10:6581
13. Hirao M, Sugimoto H, Ohno H (2000) J Electrochem Soc 147:4168
14. McEwen AB, Ngo HL, LeCompte K, Goldman JL (1999) J Electrochem Soc 146:1687
15. Garcia B, Lavallée S, Perron G, Michot C, Armand M (2004) Electrochim Acta 494:583
16. Seki S, Kobayashi Y, Miyashiro H, Ohno Y, Usami A, Mita Y, Kihira N, Watanabe M, Terada N (2006) J Phys Chem B 110:10228
17. Seki S, Ohno Y, Kobayashi Y, Miyashiro H, Usami A, Mita Y, Tokuda H, Watanabe M, Hayamizu K, Tsuzuki S, Hattori M, Terada N (2007) J Electrochem Soc 154:A173
18. Peng C, Yang L, Zhang Z, Tachibana K, Yang Y (2007) J Power Sources 173:510
19. Zhang Z, Gao X, Yang L (2005) Chin Sci Bull 50:2005
20. Bonhôte P, Dias A, Papageorgiou N, Kalyanasundaram K, Grältzel M (1996) Inorg Chem 35:1168
21. Garcia B, Armand M (2004) J Power Sources 132:206
22. Cui Q, Dewald HD (2005) Electrochim Acta 50:2423
23. Staniewicz RJ, Romero A, Broussely M, Perton F, Labat J (1992) In: Proceedings of the 35th International Power Sources Symposium. Institute of Electrical and Electronics Engineers, Inc., Piscataway, NJ, p 332
24. Zhang X, Kostecki R, Richardson TJ, Pugh JK, Ross PN Jr (2001) J Electrochem Soc 148:A1341
25. Aurbach D, Talysosef Y, Markovsky B, Markevich E, Zinigrad E, Asraf L, Gnanaraj JS, Kim H (2004) Electrochim Acta 50:247
26. Zhao L, Yamaki J -ichi, Egashira M (2007) J Power Sources 174:352
27. Choe HS, Carroll BG, Pasquariello DM, Abraham KM (1997) Chem Mater 93:69
28. Leroy S, Martinez H, Dedryvère R, Lemordant D, Gonbeau D (2007) Appl Surf Sci 253:4895
29. Dedryvère R, Laruelle S, Grugeon S, Gireaud L, Tarascon J-M, Gonbeau D (2005) J Electrochem Soc 152:A689
30. Howlett PC, Brack N, Hollenkamp AF, Forsyth M, MacFarlane DR (2006) J Electrochem Soc 153:A595
31. Moulder JF, Stickle WF, Sool PE, Bomber KD (1992) Handbook of X-ray Photoelectron Spectroscopy, Perkin-Elmer, Eden Prairie
32. Kanamura K, Tamura H, Shiraishi S, Takehara Z-I (1995) J Electroanal Chem 394:49
33. Dedryvère R, Leroy S, Martinez H, Blanchard F, Lemordant D, Gonbeau D (2006) J Phys Chem B 110:12986
34. IUPAC Chemical Data Series-No. 22 (1979) Stability constants of Metal-Ion Complexes, Part B, Organic Ligands, Compiled by Douglas D. Perrin, Pergamon Press, New York